MONITORING OF GPS PWV ASSOCIATION TO THE SOLAR ENERGETIC EVENTS DURING THE INTENSE SOLAR FLARES OF OCTOBER/NOVEMBER 2003

***Wayan SUPARTA*[1]**

ABSTRACT:
This paper monitors the influences of solar energetic events during the intense solar flares of October/November 2003 on precipitable water vapor (PWV) at Scott Base station, Antarctica for the period from 22 October to 7 November 2003. A PWV representing a climate variable to indicate the lower atmosphere has been responsive to the upper atmosphere is derived from the GPS signals and the surface meteorological data. The analysis results showed that the PWV and solar related events (EUV, proton and cosmic ray density) exhibited a strong relationship with regard a lag time of ~48 hours as preference time to observe the effects directly. PWV increased by about 0.15 mm observed during the Superstom, where EUV and solar protons increased ~24% and 16% respectively and the density of cosmic rays is decreased to 20%.

Keywords: *Monitoring, GPS PWV, Solar energetic events, Antarctica.*

1. INTRODUCTION

Application of GPS technology for such a high precision time and frequency in various fields has been expanded and has been widely recognized as an essential tool to monitor atmospheric conditions. This is done by observing the signal path delays to monitor the structure of the ionosphere (space weather) and for weather forecasting and climate research (GPS meteorology), these two aspects are the best achievement of the application of GPS technology. With the advantage of GPS to provide a continual source of accurate data, the purpose of this paper is to introduce how GPS sensing can be used to study the upper-lower atmospheric coupling. Atmospheric coupling in the Sun-Earth system is fundamental science to space physics, aerospace and satellite communication, meteorology and terrestrial climate cycle. Upper-lower atmospheric coupling studies can explain some physical mechanisms of how solar activity influences terrestrial weather/climate changes. The first initiative of this work was proposed in *Suparta (2009)*.

Although many studies have shown the solar activity affected the Earth's magnetosphere, ionosphere (*Hathaway and Wilson, 2004*), a direct influence between solar variability and climate change on atmospheric dynamics and in their physical mechanisms has proven difficult. Thus, the techniques introduced on analysis solar influence on water vapor here, are believed to have new perspective and opportunity to enlighten a solar-climate relationship. To best characterize the solar-climate relationship, a strong event is preferred as it will minimize the influence of unwanted instrumental or geophysical noise, such as the strong event is a geomagnetic storm. Geomagnetic storm tends to occur during times of geophysical or the Earth's magnetic field disturbances resulting from increases in solar activity communicated via the solar wind (*Fuller-Rowell et al., 1994*). During this

[1]*Institute of Space Science (ANGKASA), Universiti Kebangsaan Malaysia (The National University of Malaysia), 43600 Bangi, Selangor Darul Ehsan, Malaysia, E-mail: wayan@ukm.my*

event, solar flares, eruptive prominence and coronal mass ejections (CMEs) are the major causes for large geomagnetic storms (*Burlaga and Lepping*, *1997; Cane et al., 2000; Gopalswamy et al., 2005*). Solar flares are one of the most powerful and explosive of all forms of solar activity, and is the most important in terrestrial effects (*Ozguc and Atac, 1989*) involving extreme ultraviolet (EUV) radiation. The strength of flare and EUV has correlated with the size and complexity of the associated sunspot group and geomagnetic activity (*Atac and Ozguc, 1996; Dubey and Mishra, 2000*). As well, the level of geomagnetic activity at the Earth tends to follow the sunspot cycle on a yearly basis (*Webb, 1995*).

To examine solar energetic influences on lower atmosphere through production a water vapor and in order to support the IPY/IHY/ICESTAR program, Antarctica has been selected to conduct this research. It is clear shown that Antarctica due to its pristine environment offers a privileged position for the study of solar modulation on atmospheric dynamics and provides a key to explain the causes of change and prediction in the global climate systems. One key parameter in determining the climate prediction is the precipitable water vapor (PWV) derived from GPS. By proper analyzing the solar influences on PWV during high geophysical disturbances, a possibility to some extended to include the solar effects in the global climate model can be expected. In other words, this is an effort to utilize the GPS data for Sun-Earth coupling studies based on communication approach. Therefore, the global geomagnetic activity and solar indices through solar X-ray, solar flare index (SFI) and solar EUV during the major storms of 2003 ("Superstorm 2003") at Scott Base station, Antarctica is observed. The data analyses are from 22 October to 7 November 2003, which covers the period of Superstorm from 29 to 31 October of the year.

2. SOLAR ENERGETIC ACTIVITIES DURING THE INTENSE SOLAR FLARES OF OCTOBER/NOVEMBER 2003

The variation of solar-geomagnetic activity for the Superstorm 2003 including one-week before and after the storm event is presented in **Fig. 1**. The solar energetic event is characterized by geomagnetic activity: disturbance storm time (*Dst*), the estimated 3h planetary index (*Kp*) and global planetary index (*Ap*) and solar indices: solar flux index ($F_{10.7}$) and sunspot number (*SSN*). As shown in the figure, the grey background highlighted are the beginning and ending of the occurrence of the Superstorm. The storm has two distinct episodes, preceded by a high solar activity. The first storm episode occurs with the onset of the first sudden storm commencement (SSC_1) at ~06:00 UT on 29 October followed by the first *Dst* minima at ~01:00 UT with value of -363 nT and ended at ~17:00 UT on 30 October. The second storm episode occurs at ~18:00 UT on 30 October at the beginning of SSC_2, followed by second *Dst* minima at ~23:00 UT with value of -401 nT and ended at ~12:00 UT on 31 October. During this event, the *Kp* index recorded a maximum of 9 for four times; 09:00 UT and 21:00 UT on 29 October, and 21:00 UT and 24:00 UT on 30 October. The *Ap* also shown a jump abruptly from a value of 20 on 28 October to a maximum value of 189 on 29 October, and decreases dramatically to a value of 18 on 2 November when the storm subsided. Both $F_{10.7}$ and *SSN* are increases more than 250 and 200 respectively for a few days before the storm event and maintained its high values during the whole storm event.

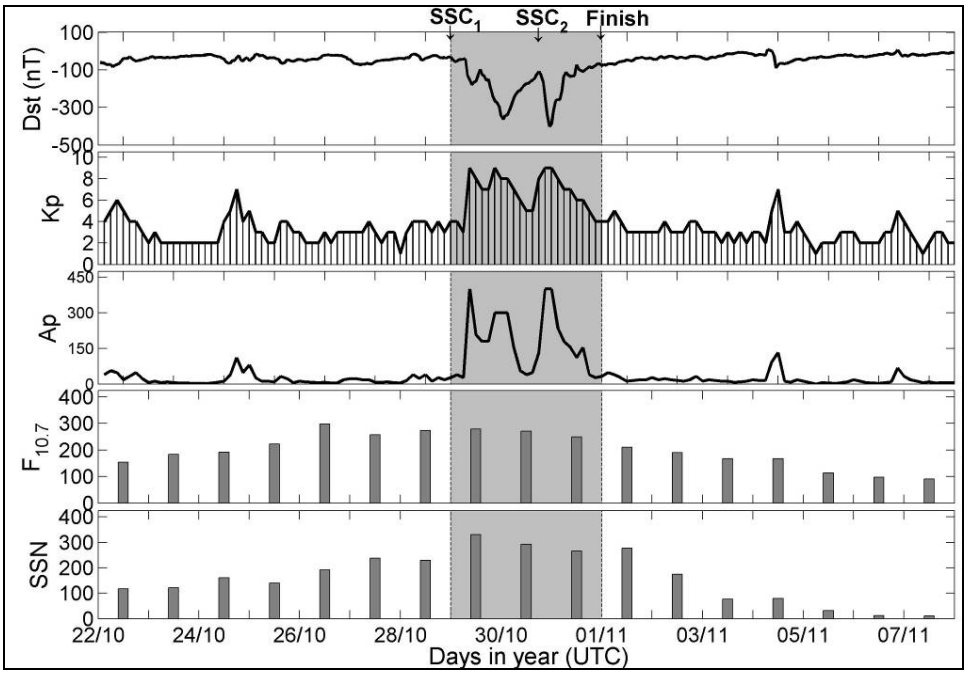

Fig. 1 The magnetic and solar indices between 22 October and 7 November 2003. The *Dst* and *Ap* indices were obtained from the World Data Center-C2 (WDC-C2) for geomagnetism, Kyoto, Japan; *SSN*, $F_{10.7}$ and *Kp* were obtained from NOAA/SEC, USA.

The intensity of X-ray flux in two bands (X_L = 1.0 to 8.0 °A) and (X_S = 0.3 to 3.0 °A) are measured by NOAA GOES-10 and GOES-12 satellites, respectively. The series of flares appeared to be originating from AR486, which produces large geomagnetic storms from AR484. There were 11 large X-class flares during this period, including an X17.2/4B flare on 28 October 2003 and an X28 flare on 4 November 2003. The X28 flare is the largest flare since GOES began its solar X-ray measurements in 1976. In October 2003, two large X-flares were recorded within this event, which are the X17.2/4B and the X10.0/2B with energies of 1.8 and 0.87 Wm^{-2}, respectively. The X17.2 flare starts active at 09:51 UT and ending at 11:24 UT on 28 October with an impulsive phase of the major energy release started at about 11:10 UT. The X10.0 flare with a peak emission was occurred at 20:49 UT on 29 October. Both flare activities take duration of 93 and 24 minutes, respectively. Prior to the major flares, other smaller flares were observed as thin ribbons of emission as reported by *Srivastava (2005)*.

Impression of solar flare activities to the solar proton events measured by NOAA GOES-12 is plotted in **Fig. 3**. There was consistency during X17.2 flare took place, the energy of protons at all levels shows a sudden increase where low bulk energy (P1) has a high intensity, while the bulk of high energy (P5) showed a lower intensity, which all have the same patterns and trends. The sudden increase of proton energy indicated by vertical dash line in the figure is coincided with sudden storm commencement (SSC). However, the last peaks of proton intensity shown an association with X28 flare activity. Further in this work, the behavior of these solar related events will be correlated with PWV variable of the lower atmosphere. The method of analysis is presented in section 3.

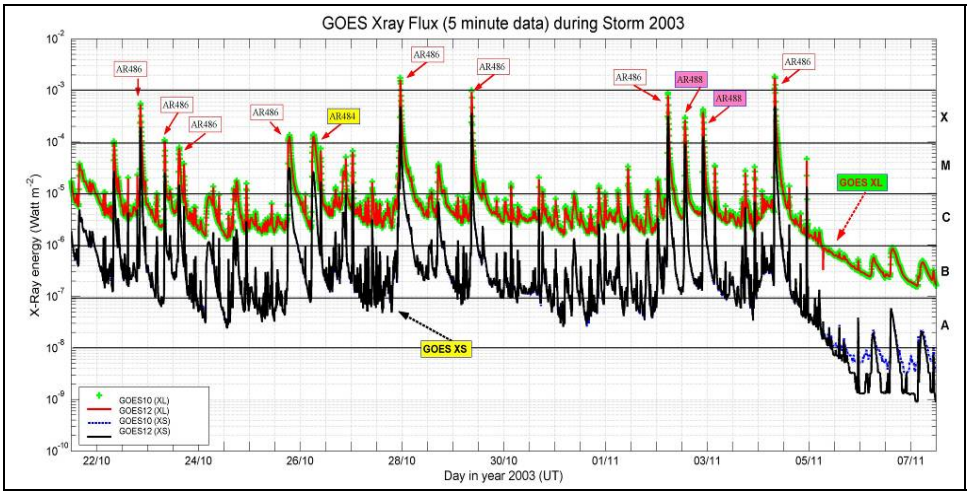

Fig. 2 NOAA GOES X-ray flare activity measured from 22 October to 7 November of 2003

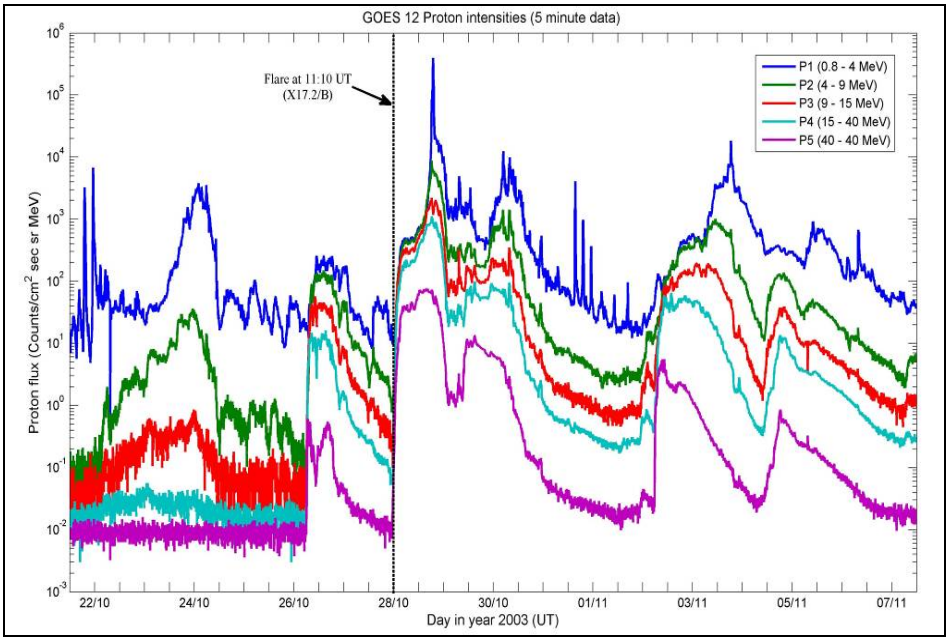

Fig. 3 Solar energetic proton intensities from NOAA GOES-12 observed from 22 October to 7 November of 2003

3. DATA AND PROCESSING

The measurement system at Scott Base station, Antarctica employed for this work consists of a GPS receiving system and a ground meteorological system. The GPS receiving system with a GPS Trimble TS5700 was installed on 18 November 2002 through the support from the Malaysian Antarctic Research Programme (MARP). The ground meteorological system is operated and managed by NIWA (National Institute of Water and Atmospheric Research Ltd, New Zealand). **Fig. 4** shows the location of a Scott Base station (SBA) and diagram block of a GPS PWV measurement system. As shown in **Fig. 4(a)**, SBA is located 1,353 km from the South Pole at Pram Point near the tip of Hut Point Peninsula in the Ross Sea region of Antarctica with Geographic: 77.85°S, 166.76°E and Geomagnetic: 79.94°S, 327.60°E position. The station is managed by the New Zealand Antarctic Institute, of Antarctica New Zealand (ANZ), and, at three kilometers away, the closest neighbor to Scott Base is the American base, McMurdo station (MCM).

In **Fig. 4(b)**, the GPS receiver was set to track GPS signals at a one-second sampling rate and the cutoff elevation angle was set to 13° to prevent the multipath effects or geophysical noise recorded in GPS data. The GPS receiver produces a data in Trimble binary format (*.dat). A Translate/Edit/Quality Check (TEQC) routine developed by UNAVCO (*http://www.unavco.org*) is then used to convert the *.dat into Receiver Independent Exchange (RINEX) format. Data are stored in the laptop in Universal Time (UT). A 30s sampling period was used in order to reduce the processing time. The RINEX files consist of five fundamental GNSS (Global Navigation Satellite System) observables: observation time, carrier phase, pseudorange, Doppler, and signal-to-noise ratio (SNR). There are two basic types of RINEX file formats in those data: the observation data and the navigation message, which are all processed to estimate the tropospheric delay. Because some signals travel through a lot of atmosphere, a mask over 30 degrees was employed in the post-processing strategy to maintain the quality of data. The basic surface meteorological data (pressure, temperature and relative humidity) at SBA was from NIWA, which employs a Campbell Scientific CR10X data logger. Mean data from the sensors were logged at 10-min intervals.

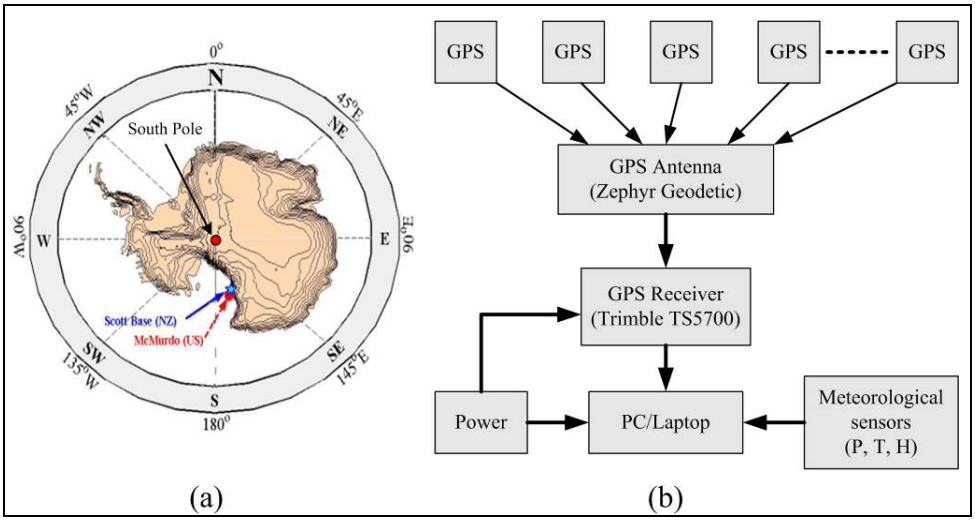

Fig. 4 Scott Base station location and diagram block for GPS PWV measurement

In the processing, the total tropospheric delay is estimated by constraining the positions of widely-spaced GPS receivers and measuring the apparent error in a position every 30s. The estimated tropospheric delay become benefit for meteorological applications, when is converted into PWV. The PWV consist of zenith tropospheric delay (ZTD), zenith hydrostatic delay (ZHD) and zenith wet delay (ZWD). On the other hand, the ZTD is calculated based on the Modified Hopfield model. The ZHD to correct the errors caused by atmospheric delays of GPS transmissions, is calculated using surface pressure measurement and precise geographic position at the GPS site. The ZWD is obtained by subtracting the ZHD from ZTD. Finally, PWV is derived from ZWD signals and a conversion factor that proportional to the weighted mean surface temperature. The weighted mean air temperature is currently estimated from a surface temperature measurement at the site. A Matlab program suite, namely the tropospheric water vapor program (TroWav) developed by the author was used to process and analyze all the above parameters. The algorithms of the TroWav include satellite elevation angle, ZTD, ZHD, ZWD and mapping function calculations. Detail of GPS derived PWV can be found in *Suparta et al. (2008)*. Because of the surface data logged at 10-min intervals, the actual PWV data (in kg/m2 or mm) at SBA has been calculated at 10-min intervals.

4. RESULTS AND DISCUSSION

The lower atmospheric variable on a daily basis represented by ZTD, PWV and surface temperature measured with GPS and meteorological sensors at SBA over the year of 2003 is plotted in **Fig. 5**. Their variation in some parts exhibits a similar pattern, but it is complicated in terms of physical manners. The ZTD value estimated from GPS fluctuates between 2.10 and 2.36 m with an average of 2.27 m. Interesting to note that ZTD is demonstrated the GPS delays above the surface of the Earth in a certain location caused by unquantified non-dispersive of the rest of the atmosphere. The PWV on the middle of figure transformed from ZTD represents the water vapor content in that location from a GPS receiver position to the top of the atmosphere. The PWV variation exhibited a seasonal variation; higher in Austral Summer (DJF) and lower in Austral winter (JJA). On a daily average, their values vary from 0.90 to 12.50 mm (~3.60 mm on average). The low PWV value indicates the dry atmosphere condition of Antarctic region. The surface temperature on the bottom of figure exhibited a similar variation to that of PWV variation, indicates surface temperature is one of the main contributors for the PWV formation. The slightly high two peaks seen between PWV and temperature during Austral winter (or between May and June shown by a double arrow) is identified as a coreless winter phenomenon. Coreless winter (kernlose winter) is developed probably due to a more frequent destruction of the low-level surface inversion in their months, rather than a temporary increase in the level of warm air advection into the region (*Thompson, 2006*). This phenomenon caused by the much smaller absorbency of solar radiation. The temperature trend relatively increases for a few months after the spring leading to a maximum early in the winter compared to the surrounding oceans.

From existing lower atmosphere variable measured with GPS, the association between solar activity and PWV during the period of Superstorm is presented. **Fig. 6** shows the SFI, EUV, solar cosmic ray density (SCR), solar energetic particle (SEP) and PWV variation during the period of observation. On the top of the figure, SFI is representing the total energy emitted by the Sun, which well correlated with the geomagnetic activity indices. The peak of SFI for Southern Hemisphere region was measured maximum of 116 on 28 October 2003. This value is associated with the occurrence of X17.2/4B flare.

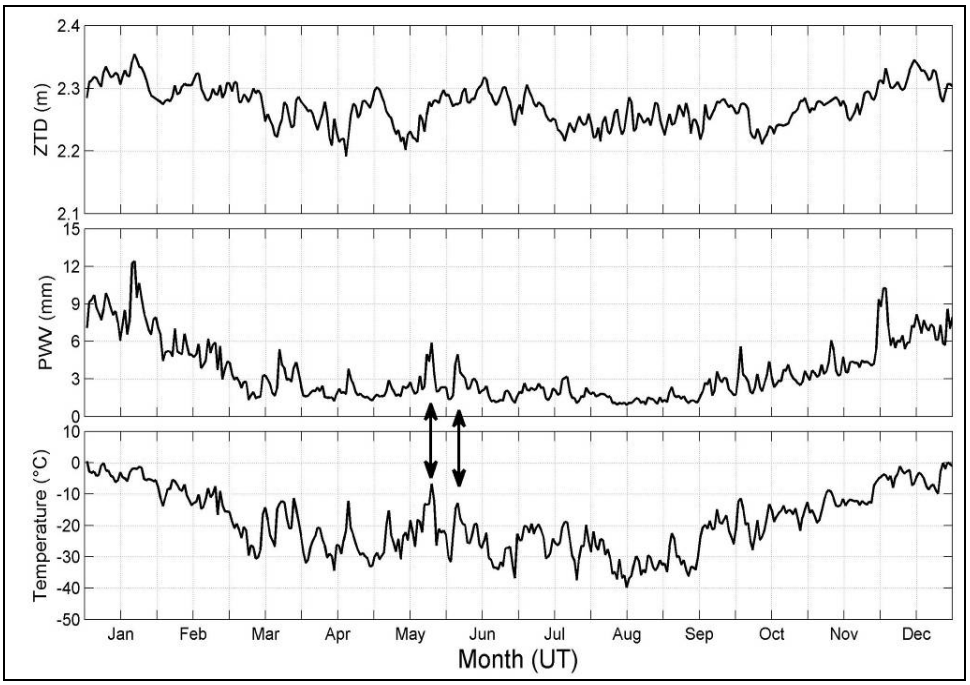

Fig. 5 The lower atmospheric variation (ZTD, PWV and Temperature) on a daily basis over the year of 2003 observed at Scott Base station, Antarctica

The maximum value of about 144 for full disk is a summation of the SFI for Southern Hemisphere and Northern Hemisphere regions. The second panel of **Fig. 6** presents solar EUV (λ = 10-120 nm) radiation, which is one of the primary energy inputs to the thermosphere and ionosphere. Both SFI and EUV variation on a daily basis is correlated well to each other. One interesting result for the EUV flare variations is that the EUV variations for an X17/4B flare range from a factor of about 50 shortward of 10 nm to about 10% for the Mg II 280 nm emission. The third panel of **Fig. 6** shows the percentage of SCR measured in a 5-min interval from near-polar neutron monitors at McMurdo and South Pole stations in Antarctica. The SCR peak at both stations shows a jump abruptly and the highest fluxes of SCR nuclei in this series arrived after the flare X17.2/4B observed at 09:51–11:24 UT on 28 October, which were modulated by a strong shock wave (SW). Then they dropped and increase again following the phase of *Dst*, or inverse relationship with *SSN*. The fourth panel of **Fig. 6** shows the natural logarithmic of solar energetic particle (SEP) for electrons and protons, which are measured in intervals of 1-hour from NOAA GOES. The significant enhancement of proton fluxes in both energy intervals was observed in the impulsive of X17.2 flare at 19:50 UT, which the first arrival of SCR from this flare was observed at 12:46 UT for protons with energies 0.7–4 MeV. The arrival of particles is faster and reached their maximum at ~18 UT. This increase is associated with SW. On the bottom of **Fig. 6** presents the PWV measurement from GPS in a 10-min interval at SBA. The PWV variation in the date before and after the superstorm identified, has shown fluctuates following the Earth's surface conditions. The low value of PWV during the event is associated with season transition from spring to Austral summer. During the period of superstorm, a response of PWV to SEP protons is clear with a linear relationship.

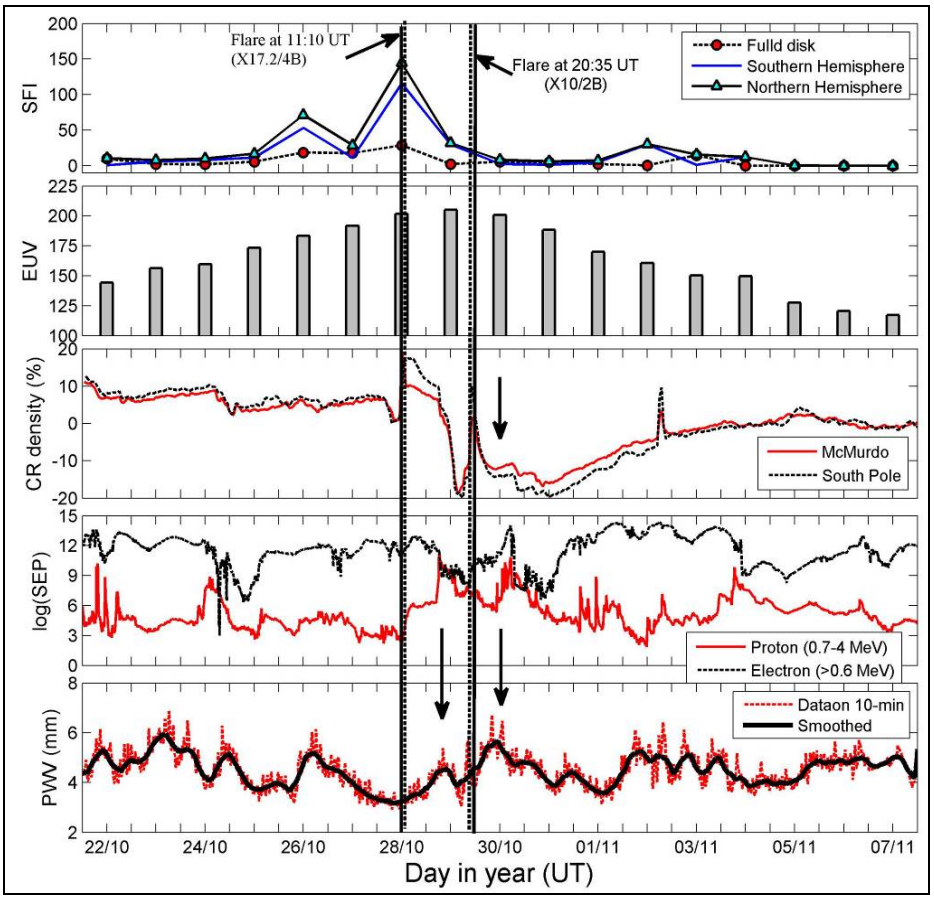

Fig. 6 Solar energetic activity and PWV variation observed from 22 October to 7 November of 2003. The vertical solid line shows the time occurrence of flare activity (X17.2/4B and X10/2B), the vertical dash line shows the shock time wave of both flares, and down arrows shows the association between solar activity of upper atmosphere and PWV of the lower atmosphere.

The association between solar energetic events with PWV during the period of Superstorm can be explained as follows. A geomagnetic storm brings prominences on the structure of the ionosphere characterized by solar flares. Solar EUV connected to the SFI, which is along the Supertorm increased by about 20% compared to their average value during the observation period. The increases of EUV could be due to absorption of EUV photons. The EUV is responsible for most of the heating in the thermosphere (*Viereck et al., 2001*). The EUV photons also to ionize the neutral atmosphere, forming the ionosphere, and with intense of solar energetic particle, the influence of EUV on the atmospheric dynamic as well as the lower atmosphere is possible. On the other hands, solar EUV is responsible for approximately 80% of thermospheric heating, except during major geomagnetic disturbances when Joule heating dominates. As shown in the figure, before SFI reached to a maximum, SCR together with SEP protons on 28 October showed a sudden increase, and PWV measured start to increase at this time. During SFI and EUV maximum, SCR start to decrease and there is matched between SEP electrons and protons,

PWV is increased at that time. When SFI and EUV start to decrease, SCR jump significantly and SEP separated increases, and clear shown that the PWV had increased (~1 day response after the peak of EUV or SCR). During this process, EUV photons are intense absorbed by neutral atmospheric O_2 and N_2, which raise the kinetic temperature of the atoms and molecules (*Tobiska, 2003*). Increased of absorption activity resulted in a net increase in any particular neutral species densities for a given altitude layer. With acting of SCR (Forbush decrease), the formation of H_2 process with increased in altitude caused the autocatalytic water vapor formation insufficient energy to production of H_2O, and as a result PWV is increased. From the figure, it may be concluded that the solar energetic phenomenon is associated with electromagnetic coupling of velocity of solar wind streams and interplanetary magnetic field (IMF). Large solar flares, together with coronal mass ejection (CME) can produce copious quantities of energetic particles, X-rays, gamma-rays, ultraviolet (UV) light bursts, as well as super fast solar wind flows, and they have the most extreme effects on the terrestrial environment. Based on the timing of transfer energy of the Sun and its instantaneous propagation through the Earth-ionospheric wave-guide, the intensity PWV peak on 30 October (~2 days after peak time of X17.2 flares in **Fig. 2**) was identified influenced by flare activities through EUV photons and deactivation of SCR.

From monitoring the event, the association between solar related events and PWV can be summarized as follows. The maximum value of PWV during Superstorm is 6.87 mm, or increased of about 0.15 mm (~35% compared to their mean value during the observation period). PWV is low of ~0.05% before the storms occur. Before and after the Superstorm, the PWV variation still varies, which may be influenced by surface temperature domination (see **Fig. 4**). Looking at the direct influence of solar activity with the same time of occurrence from top to bottom during X17.2 flare event, PWV profile was dropped to a minimum of 3.2 mm on 28 October or opposite relation to the SFI. During this time, the impulsive of SCR density took place and energy spectrum of protons slightly increased. One day later, when SEP spectrum for electron and protons meet together (with a proton increase of 16%), the SCR density then drops drastically to about -20% and solar EUV reach to a maximum intensity followed by PWV increase to about 15%. After the second sudden increase of SCR (~12 hrs later), SEP spectrum increased and PWV reach to a maximum. However, the fact of all the process above is complicated. The radio propagation paths of the signals traveling from space to ground are taking time. Under a normal condition, the particles travel with solar wind speeds between 300 and 800 km/s and reach the Earth after 2.2 to 5.8 days (*Suess and Tsurutani, 2000*). Based on these facts, we need to define appropriate time preference to clarify how solar related events affected the lower atmosphere.

CONCLUSION

The monitoring and analysis of solar energetic phenomena influence on the production of PWV at Scott Base station during the major storms of 2003 ("Superstorm 2003") which covers the period from 29 to 31 October of the year are presented. The PWV increase or decrease at Scott Base station during Superstorm shows affected by variations of EUV, SEP protons and CR density. This clear indicated that solar activity affects the GPS signals. On the other hand, the analysis of PWV association with solar related events was complicated due to lag time of the geophysical events with an increase or decreasing the PWV phase is different in preferred time. Therefore, to clarify a direct influence of solar activity to the lower atmosphere in short-term data and other events require appropriate time definition to prove the proposed method and is remaining a topic of further interest.

REFERENCES

Atac T., Ozguc A., (1996), *North-south asymmetry in the solar flare index*, Solar Physics, Vol. 166, pp. 201-208.

Burlaga L.F., Lepping R.P., (1997), *The causes of recurrent geomagnetic storms*, Planetary Space Phys., Vol. 25, pp. 1151.

Cane H.V., Richardson I.G., St. Cyr O.C., (2000), *Coronal mass ejections interplanetary ejecta and geomagnetic storms*, Geophys. Res. Lett., Vol. 27, pp. 3591.

Dubey S.C., Mishra A.P., (2000), *Flare index of solar activity and global geomagnetic variability*, Current Science, Vol. 78, pp. 1365-1366.

Fuller-Rowell T.J., Codrescu M.V., Moffett R.J., Quegan S., (1994), *Response of the thermosphere and ionosphere to geomagnetic storms*, J. Geophys. Res., Vol. 99, pp. 3893-3914

Gopalswamy N., Yashiro S., Michalek G., Xie H., Lepping R.P., Howard R.A., (2005), *Solar source of the largest geomagnetic storm of cycle 23*, Geophys. Res. Lett., Vol. 32, L12S09, DOI: 10.1029/2004GL021639

Hathaway D.H., Wilson R.M., (2004), *What the sunspot record tells us about space climate*, Solar Phys., Vol. 224, pp. 5-19

Ozguz A., Atac T., (1989), *Periodic behavior of solar flare index during solar cycles 20 and 21*, Solar Physics, Vol. 123, pp. 357-365

Srivastava N., (2005), *Predicting the occurrence of super-storms*, Ann. Geophys. Vol. 23, No. 9, pp. 2989-2995

Suparta W., Abdul Rashid Z.A., Mohd Ali M.A., Yatim B., Fraser G.J., (2008), *Observations of Antarctic precipitable water vapor and its response to the solar activity based on GPS sensing*, Journal of Atmospheric and Solar-Terrestrial Physics, Vol. 70, pp. 1419-1447

Suparta W., (2009), *Application of GPS sensing technique for sun-earth coupling studies,* Geographia Technica Nr.2/2009, pp. 94-105, ISSN 2065-4421

Suess S.T., Tsurutani B.T., (2000), *Solar wind to appear in Ensclopedia of atmospheric sciences*, http://trs-new.jpl.nasa.gov/dspace/bitstream/2014/15128/1/00-1139.pdf

Tobiska W.K., (2003), *Forecast E10.7 for Improved LEO Satellite Operations*, J. Spacecraft Rock, Vol. 40, No. 3, pp. 405-410.

Thompson D.C., (2006), *The coreless winter at Scott Base, Antarctica*, Quart. J. Roy. Meteor. Soc., Vol. 95, Issue 404, pp. 404 – 407

Viereck L., Puga L., McMullin D., Judge D., Weber M., Tobiska W.K., (2001), *The Mg II Index: A Proxy for Solar EUV*, Geophys. Res. Lett., Vol. 28, No. 7, pp. 1343-1346

Webb D.F., (1995), *Solar and geomagnetic disturbances during the declining phase of recent solar cycles*, Adv. Space. Res., Vol. 16, pp. 57-69.